

Monitoring of geophysical processes in the area of western Herzegovina by satellite observations

Marin Vrankić

J.P. „Elektroprivreda HZ HB“ d.d. Mostar, M.Sc, marin.vrankic96@gmail.com

Marijan Grgić

University of Zagreb, Faculty of Geodesy, Ph.D, marijan.grgic@geof.unizg.hr

Tomislav Bašić

University of Mostar, Faculty of Civil Engineering, Architecture, and Geodesy, prof. Ph.D,
tomislav.basic@fgag.sum.ba

Abstract: Developments in sensor technology called Synthetic Antenna Radar (SAR) and associated data processing software have helped satellite radar interferometry (InSAR), a method that uses multiple SAR images of the same area collected from satellites, to become a widely used method for estimating soil deformation as well as other geophysical processes, because it provides millimeter precision with great spatial coverage. The paper deals with 24 Sentinel-1A images for the area of western Herzegovina, taken during 2020, and determined the average speeds of vertical displacements using the SNAP program (Sentinel Application Platform). Vertical displacements of ± 10 millimeters were recorded, while the mean annual displacement velocities were 8 millimeters in the vertical direction, without taking into account the correction for the influence of horizontal displacements. The first results in the study area indicate a trend of ground movement, but due to several types of atmospheric corrections, geomorphological characteristics of the study area and lack of in-situ measurements for comparison, external evaluation of the reliability of deformations will have to be assessed in future studies.

Key words: satellite interferometry, Sentinel-1, deformations, vertical displacement

Praćenje geofizičkih procesa na području zapadne Hercegovine satelitskim opažanjima

Sažetak: Razvoj tehnologije senzora koji se naziva radar sa sintetičkom antenom (SAR) i pripadajućeg softvera za obradu podataka pomogli su da satelitska radarska interferometrija (InSAR), metoda koja koristi više SAR snimki istog područja, prikupljenih sa satelita, postane široko korištena metoda za procjenu deformacije tla kao i drugih geofizičkih procesa, jer pruža milimetarsku preciznost uz veliku prostornu pokrivenost. U radu su obrađene 24 Sentinel-1A snimke za područje zapadne Hercegovine, napravljene tijekom 2020. godine te su određene srednje brzine vertikalnih pomaka koristeći program SNAP (Sentinel Application Platform). Zabilježeni su vertikalni pomaci iznosa ± 10 milimetara dok srednje brzine pomaka na godišnjoj razini iznose 8 milimetara u vertikalnom smjeru, bez uzimanja u obzir korekcije za utjecaj horizontalnih pomaka. Ostvareni prvi rezultati na području istraživanja ukazuju na određeni trend gibanja tla, ali zbog više vrsta provedenih atmosferskih korekcija, geomorfoloških karakteristika područja istraživanja te pomanjkanja in-situ mjerenja za potrebe usporedbe, morati će se vanjska ocjena pouzdanosti dobivenih deformacija procijeniti u budućim istraživanjima.

Ključne riječi: satelitska interferometrija, Sentinel-1, deformacije, vertikalni pomaci

Vrankić, M., Grgić, M., Bašić, T.

Monitoring of geophysical processes in the area of western Herzegovina by satellite observations

1. INTRODUCTION

Satellite imaging radars began to play an important role in remote sensing in the late 1970s. The first missions demonstrated that Synthetic Aperture Radar (SAR) is able to reliably map the Earth's surface and acquire information about its physical properties, such as topography, morphology or roughness. SAR is a system that uses electromagnetic pulses with microwave frequencies, making it possible to acquire unique images that represent electrical and geometric properties of the surface in almost all weather conditions. SAR is an active system that collects data in daylight and at night.

The use of space SARs as interferometers became available in the 1980s, when the first civilian satellite mission, Seasat, was launched in 1978 and in just 100 days collected plenty of data and demonstrated the full potential of the technology (Hanssen, 2001). It was only after the ESA's (European Space Agency) ERS-1 satellite was launched in 1991 that this type of measurement caught the eye of the wider scientific community. InSAR technology has been extensively and successfully studied and its results are published in many papers.

By reflecting satellite radar signals from the Earth's surface in the same or similar orbits and looking at differences between images, interferometric radar with synthetic antenna can detect small differences in distance between its position and the ground resulting from geophysical processes in a time interval. InSAR (Interferometric Synthetic Aperture Radar) displays spatial deformation patterns and, in combination with field measurements, provides insight into a wide range of natural processes relevant to Earth sciences (Massonnet et al., 1993).

A digital SAR image can be viewed as a mosaic of pixels. Each pixel carries information about the amplitudes and phases of microwave radiation reflected from all scatterers (such as rocks, buildings, vegetation) within the corresponding resolution cell projected on the ground. The amplitude depends on the roughness and it is usual that exposed rocks and urban areas show strong amplitudes, while smooth flat surfaces (such as water) show low amplitudes. The phase information of the image is directly related to the distance between the observed terrain and the sensor on the satellite. By calculating the differences in phases (interferogram) between the two data sets, it is possible to determine ground displacements that have occurred in the time between data acquisitions.

The objective of this paper is to study the potential of InSAR measurements, to learn how to acquire data and process them in the program SNAP (Sentinel Application Platform) and on the basis of theoretical knowledge to analyze the processed data. Western Herzegovina, which is interesting to us, was chosen as the study area, and the time period is 2020.

2. DATA ACQUISITION

The images were downloaded through the Alaska Satellite Facility (ASF, URL 2), a data processing institution that is also a ground-based satellite tracking station within the Geophysical Institute at the University of Alaska at Fairbanks. ASF has developed and deployed the Vertex user interface to highlight the contents of the pre-processed ASF DAAC SAR database. Vertex is an intuitive user interface that facilitates the search for and visualization of ASF DAAC datapool assets, delivery of relevant metadata on the images, and bulk delivery of those ASF data (URL 2). Vertex is designed to familiarize users with SAR data without requiring any prior knowledge of SAR platforms, beam methods, or processing parameters. The search is performed by marking the area of interest and selecting the observation interval, satellite mission, satellite, data type, polarization, acquisition method and relative orbit number. Vertex

Vrankić, M., Grgić, M., Bašić, T.

Monitoring of geophysical processes in the area of western Herzegovina by satellite observations

does not have a data download limit as the Copernicus Open Access Hub (ESA) has a limit of two images per day. For the purposes of this paper, Sentinel-S1A satellite data were used, with IW acquisition mode and VV polarization, and relative orbit 73 in the period from January to December 2020. The area of interest is the part of the area of western Herzegovina selected using the boundary coordinates (Figure 1).



Figure 1. Red square indicates the footprint of the antenna operating in IW mode while yellow square indicates the area that will be treated below

Twenty-four images from 12 January 2020 to 13 December 2020 were used, two images per month, the minimum time interval between most images is 12 days due to time errors. The image parameters are shown in Table 1. B_{temp} is the data on how many days have passed from the acquisition of the image to the so-called main image which in this case is 10 July 2020 (mst). B_{\perp} is the geometric baseline, and H_{amb} is the altitude ambiguity, defined as the variation in terrain height that causes phase changes of 2π . In Table 1, it is obvious that altitude ambiguity decreases with increasing baseline. Figure 2 shows the simplified geometry of the satellite at the time of image acquisition.

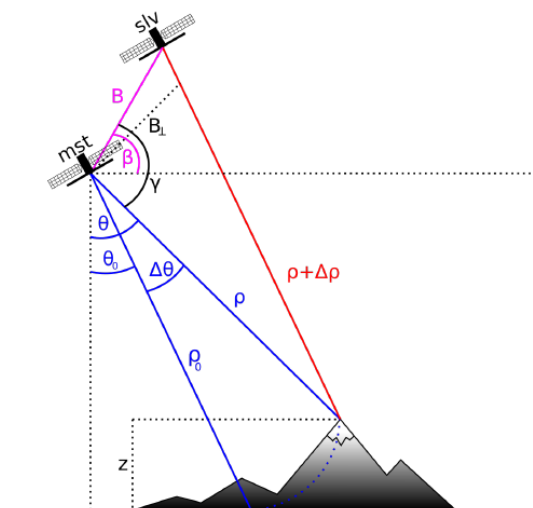


Figure 2. Geometry of repeated overpass for calculating the displacement using the relative position of the sensor. mst and slv are sensor positions at two different time points, B interferometric baseline, B_{\perp} vertical baseline, ρ and $\rho + \Delta\rho$ distance from target n2

Vrankić, M., Grgić, M., Bašić, T.

Monitoring of geophysical processes in the area of western Herzegovina by satellite observations

For the purpose of displacement monitoring, it is preferable that the B_{\perp} values are low because the sensitivity to topography is reduced. The Doppler centroid frequency is the frequency shift from the target point which is at the center of the antenna beam. For an ideal SAR system, its value should be zero, but it is practically different from zero because of the look angle which is not zero and the sensor path. The difference in frequencies of the Doppler centroids Δf_{DC} between individual images causes decorrelation in the azimuth direction. The coherence factor decreases linearly with increasing Δf_{DC} (Hanssen 2001).

Table 1. Parameters of the images used

| Acquisition date | B_{\perp} [m] | Btemp [day] | Hamb [m] | Δf_{DC} [Hz] |
|------------------|-----------------|-------------|----------|----------------------|
| 12.01.2020 | 34.35 | 18 | -462.32 | 2.62 |
| 24.01.2020 | 41.10 | 168 | -386.37 | -4.36 |
| 05.02.2020 | 38.94 | 156 | -407.83 | 1.07 |
| 17.02.2020 | -24.07 | 144 | 659.72 | 5.29 |
| 12.03.2020 | 50.72 | 120 | 313.12 | 0.39 |
| 24.03.2020 | 6.68 | 108 | -2376.53 | -0.84 |
| 05.04.2020 | 14.71 | 96 | -1079.76 | 0.73 |
| 17.04.2020 | -61.09 | 84 | 259.96 | -0.94 |
| 11.05.2020 | -26.75 | 60 | 593.62 | 1.79 |
| 23.05.2020 | -26.53 | 48 | 598.47 | -1.46 |
| 04.06.2020 | 80.83 | 36 | -196.47 | 2.13 |
| 28.06.2020 | -30.37 | 12 | 522.86 | 1.01 |
| 10.07.2020 (mst) | 0.00 | 0.00 | | 0.00 |
| 22.07.2020 | -11.26 | -12 | 1410.83 | 0.27 |
| 03.08.2020 | 21.65 | -24 | -733.65 | 2.07 |
| 15.08.2020 | -72.08 | -36 | 220.30 | -1.38 |
| 08.09.2020 | -92.37 | -62 | 171.91 | -1.00 |
| 20.09.2020 | -21.12 | -72 | 752.06 | 3.01 |
| 02.10.2020 | 28.91 | -84 | -549.21 | 4.72 |
| 14.10.2020 | -13.42 | -96 | 1183.60 | 5.51 |
| 07.11.2020 | -55.73 | -120 | 284.97 | 0.32 |
| 19.11.2020 | -61.14 | -132 | 259.72 | 0.51 |
| 01.12.2020 | 94.50 | -144 | -168.04 | 0.78 |
| 13.12.2020 | 70.16 | -156 | -226.35 | -1.06 |

3. DATA PROCESSING

Images were processed using the program Sentinel Application Platform (SNAP). Instructions and processing steps are taken from the TOPS Interferometry Tutorial (URL 3), created by Andres Braun from the University of Tübingen. Processing steps refer to image pairs, which means that 23 interferograms were created from 24 images. An interferogram is formed by cross multiplying the reference image with the related secondary image. The amplitude of both images is multiplied, while the phase represents the phase difference between the two images. The interferometric phase of each SAR image pixel would depend only on the difference in the travel paths from each of the two SARs to the considered resolution cell. Accordingly, the computed interferogram contains phase variation φ from several contributing factors, φ^{flat} is the flat earth phase contained in the measurement due to the earth's curvature and is removed by DEM (Digital Elevation Model), φ^{topo} topographic phase or relief surface phase, φ^{disp} ground displacement between the two images, the φ^{atm} contribution of the atmosphere to the phase

Vrankić, M., Grgić, M., Bašić, T.

Monitoring of geophysical processes in the area of western Herzegovina by satellite observations

signal, the φ^{orbit} contribution due to the change in platform's orbit and φ^{noise} the effect of phase noise. Differential SAR interferometry tries to estimate the contribution from the earth's surface φ^{flat} and φ^{topo} , which is considered equal for both image acquisitions, and remove them from the interferogram, so the remaining phase variations can be attributed to surface elevation changes between both image acquisition moments (Equation (1)).

$$\varphi = \varphi^{\text{flat}} + \varphi^{\text{topo}} + \varphi^{\text{disp}} + \varphi^{\text{atm}} + \varphi^{\text{orbit}} + \varphi^{\text{noise}} \quad (1)$$

This works best if atmospheric contributions and other noise are kept as small as possible because they are difficult to model. Therefore, it is advisable to use images from the dry season and with small perpendicular baseline and smaller time intervals between images (min. 12 days). In addition to the interferometric phase, the coherence between the reference and the secondary image is estimated as an indicator of the quality of the phase information. Basically, it shows if the images have strong similarities and are therefore useful for interferometric processing. Loss of coherence can result in poor interferometric results, and is caused by temporal (over vegetation and water surfaces), geometric (errors or inaccuracies in orbit metadata) and volumetric decorrelation (potential scattering mechanisms of structures such as complex vegetation). Coherence is calculated as a separate raster band and shows how similar each pixel is between the secondary and reference images on a scale of 0 to 1. Areas of high coherence will look bright and areas with poor coherence will be dark. As topographic phase removal was applied, the interferogram should then contain only variations from displacement, atmosphere, and noise. Coherence is displayed in a rainbow color scale, ranging from $-\pi$ to $+\pi$. The patterns, also called fringes represent a full 2π cycle and appear in the interferogram as cycles of arbitrary colors, with each cycle representing half of the sensor wavelength. The relative ground movement between two points is later obtained by counting the fringes and multiplying by half of the wavelength. The denser the fringes, the greater the ground displacements. The coherence shows the areas where the phase data are coherent, which means that they can be used to measure deformations or topography (without removing the topographic phase). While urban areas and agricultural land are shown in white and show high coherence values (above 0.6), forest areas are dark and have low coherence (below 0.3). Accordingly, phase information on forest areas is not useful here. If low coherence areas are too dominant in the image, the later phase unwrapping will fail and produce faulty or random results.

4. ANALYSIS OF RESULTS

For the purposes of this paper, the displacement values of individual interferograms are not important because they are valid for a short period of time and are affected by atmospheric errors and unwrapping errors. Using the Create Stack option, it is necessary to stack 23 products showing the shifts in the map projection, which makes it possible to subsequently calculate the arithmetic mean of pixel shift values for 2020. Atmospheric errors and phase unwrapping errors are considerably reduced in this way. Figure 3 shows the product of the arithmetic mean of shifts created by processing the data time series for 2020. The darker parts of the image show places where the displacements are very small or negligible, and the light parts where the displacements are larger than 1.5 cm. These darker parts are related to arable land near Grude, Drinovci and Klobuk and the white to a mountainous area between the mountains Čabulja and Čvrstica, where, logically, larger displacements were measured.

Vrankić, M., Grgić, M., Bašić, T.

Monitoring of geophysical processes in the area of western Herzegovina by satellite observations

Table 2. Table view of statistical indicators of image quality

| | |
|--------------------------|-----------|
| Total number of pixels | 8 934 768 |
| Minimum | 0.0000 |
| Maximum | 0.0247 |
| Mean | 0.0108 |
| Standard deviation | 0.0015 |
| Median | 0.0107 |
| Coefficient of variation | 14% |
| Maximum error | 0.00002 |

The table shows the total number of pixels, the minimum and maximum values of displacement for these pixels, the mean or arithmetic mean of all displacements is 11 mm, which is more than expected due to pixels with values greater than 2 cm which we consider unreliable, standard deviation is 1.5 mm, coefficient of variation is the ratio of standard deviation to mean value, this value of coefficient of variation of 14% is satisfactory because data sets with coefficient of variation of over 30% are considered unreliable.

A large number of high-quality input images as well as appropriate processing methods were used in this paper in order to achieve satisfactory data. Based on graphical and statistical indicators and some knowledge of the relief of the area used, the obtained results can be considered reliable, but to a certain extent. The only way to correctly verify the results is to compare them with field measurements such as satellite positioning or leveling measurements. Eventually, the reliability of data can be increased only by using a coherence mask or by removing pixels with a coherence value of less than 0.3.

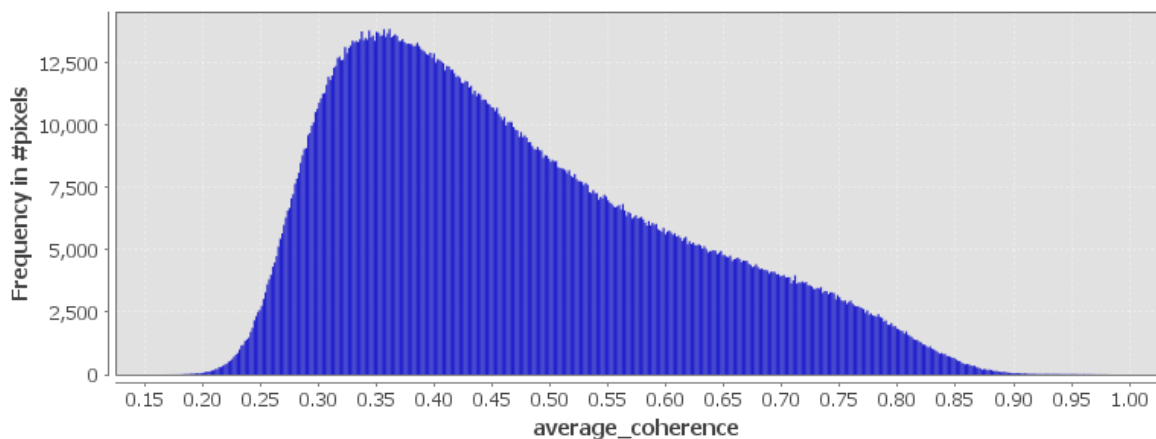


Figure 5. Histogram of average coherence for image pairs from 2020 5

It is obvious in Figure 5 that a significant number of pixels still have a coherence of less than 0.3, therefore a coherence threshold is used to graphically separate unreliable data (Figure 5).

Vrankić, M., Grgić, M., Bašić, T.

Monitoring of geophysical processes in the area of western Herzegovina by satellite observations



Figure 6. Smaller image area after applying the coherence mask (m)6

Figure 6 shows that the displacement values are retained only for parts of the surface with better scatterer characteristics, such as a hillside with less vegetation, while measurements with more vegetation or water surfaces are left out. After extracting pixels with a coherence of less than 0.3 from the data set, statistical indicators suggest that the mean value of the vertical displacement has decreased to 8 millimeters, while the maximum value is 2 cm.

5. CONCLUSION

Thanks to the Copernicus initiative and advances in technology and processing of satellite systems, the use of satellite data for scientific purposes has grown significantly since 2016. In addition to the great contribution of the European Space Agency, which provided free access to data, in the last six years the scientific community has managed to raise the level of existing methods and programs and create new methods of data processing. This paper uses deformation analysis based on SAR measurements, which are most interesting for geophysical geodesy, but there are other types of satellite measurements such as optical, infrared, LiDAR (Light Detection and Ranging) or gravimetric satellite measurements that may be useful to surveyors. The main disadvantages of InSAR measurements are their susceptibility to atmospheric errors, inability to work in real time and the fact that the displacement values are related to pixels rather than points, which is not suitable for certain applications. However, the excellent price-quality ratio, high spatial coverage, sub-centimeter precision make this technology one of the most attractive remote sensing methods.

In this paper, 24 images from 2020 were used for the area of western Herzegovina, which is still understudied in terms of geophysical processes. By analyzing the results, it was concluded that most pixels have displacements in the direction between the sensor and the ground ± 10 mm, but using this method it is difficult to conclude what the effect of horizontal ground displacements is. The obtained results on vertical displacement can be explained in terms of some basic knowledge of the geological and tectonic properties of the observed

Vrankić, M., Grgić, M., Bašić, T.

Monitoring of geophysical processes in the area of western Herzegovina by satellite observations

area, but it is difficult to reach absolute conclusions about the reliability of the results obtained by these satellite measurements without high-quality terrestrial measurements. A better picture of the geophysical processes can be obtained by using images from several years as well as by carefully selecting images with better coherence. Due to high temperatures and the stone cover of western Herzegovina, the decrease in the quality of images in the summer period is significantly influenced by atmospheric errors. In addition to having terrestrial measurements, it would be optimal to test other algorithms such as PS-InSAR (Persistent Scatterers InSAR), which relies on PS (Persistent Scatterers), pixels with consistent scatter properties, and SBAS (Short BAseline Subset), and a more general approach that uses pixels with DS (Distributed Scatterers), and then to compare the results.

As data processing methods and algorithms become more and more automated and user-friendly in recent years, this trend is expected to continue in the coming years.

REFERENCES

1. Andrade, E.: Doppler and the Doppler effect. *Endeavour* 18 (69), 14–19., 1959
2. Benallegue, M., Taconet, O., Vidal-Madjar, D. & Normand, M.: The use of radar backscattering signals for measuring soil moisture and surface roughness. *Remote Sensing of Environment* 53 (1), 61–68., 1995
3. Bender, J.: InSAR vremenski nizovi u praćenju vertikalnih pomaka Zemljine kore (InSAR time series in monitoring the vertical displacements of the Earth's crust), graduation thesis, Faculty of Geodesy, Zagreb, 2018
4. Braun, A.: Radar satellite imagery for humanitarian response - bridging the gap between technology and application. Tübingen: University of Tübingen, 2019
5. Cindrich, I., Marks, J. & Klooster, A.: Coherent optical processing of Synthetic Aperture Radar data. In: Vatz, B. W. (Ed.): SPIE 0128. Effect Utilization of Optics in Radar Systems, 27 September 1977, Huntsville, 128–143, 1977
6. Daida, J. M., Onstott, R. G., Bersano-Begey, T. F., Ross, S. J. & Vesecky, J. F.: Ice roughness classification and ERS SAR imagery of Arctic sea ice: Evaluation of feature-extraction algorithms by genetic programming. In: IGARSS 1996. IEEE International Geoscience and Remote Sensing Symposium, 27-31 May 1996, Lincoln, NE, USA, 1520–1522., 1996
7. Derooin, J.-P., Company, A. & Simonin, A.: An empirical model for interpreting the relationship between backscattering and arid land surface roughness as seen with the SAR. *IEEE Transactions on Geoscience and Remote Sensing* 35 (1), 86–92., 1997
8. Dong, Y., Forster, B. C. & Ticehurst, C.: Radar backscatter analysis for urban environments. *International Journal of Remote Sensing* 18 (6), 1351–1364., 1997
9. Ferretti, A., Monti-Guarnieri, A., Prati, C., Rocca, F., Massonnet, D.: *InSAR Principles: Guidelines for SAR Interferometry Processing and Interpretation*, 2007
10. Gatelli, F., Guarnieri, A. M., Parizzi, F., Pasquali, P., Prati, C. & Rocca, F.: The wavenumber shift in SAR interferometry. *IEEE Transactions on Geoscience and Remote Sensing* 32 (4), 855–865., 1994
11. Gauthier, Y., Bernier, M. & Fortin, J.-P.: Aspect and incidence angle sensitivity in ERS-1 SAR data. *International Journal of Remote Sensing* 19 (10), 2001–2006., 1998
12. Hanssen, R. F.: *Radar interferometry: data interpretation and error analysis (Vol. 2)*. Springer Science & Business Media, 2001

Vrankić, M., Grgić, M., Bašić, T.

Monitoring of geophysical processes in the area of western Herzegovina by satellite observations

13. Hooper, A., Segall, P., Zebker, H.: Persistent scatterer interferometric synthetic aperture radar for crustal deformation analysis, with application to Volcán Alcedo, Galápagos. *J. Geophys. Res. Solid Earth* 112:B07407., 2007
 14. Hooper, A., Zebker, H., Segall, P., Kampes, B.: A new method for measuring deformation on volcanoes and other natural terrains using InSAR persistent scatterers. *Geophysical Research Letters*, 31(23), 2004
 15. Höser, T. Analysing the Capabilities and Limitations of InSAR using Sentinel-1 Data for Landslide Detection and Monitoring. Master's Thesis, Department of Geography, University of Bonn, Bonn, Germany, 2018
 16. Massonnet, D., Feigl, K. L.: Radar interferometry and its application to changes in the Earth's surface. *Reviews of Geophysics*, 36(4), 441-500., 1998
 17. Massonnet, D., Souyris, J. C.: *Imaging with synthetic aperture radar*. CRC Press, 2008
 18. Massonnet, D., Rossi, M., Carmona, C. et al.: The displacement field of the Landers earthquake mapped by radar interferometry. *Nature* 364, 138–142., 1993
 19. Richards, J. A.: *Remote sensing with imaging radar*, Heidelberg, New York: Springer, 2009
 20. S. L. Ullo et al.: "Application of DInSAR Technique to High Coherence Sentinel-1 Images for Dam Monitoring and Result Validation Through In Situ Measurements," in *IEEE Journal of Selected Topics in Applied Earth Observations and Remote Sensing*, vol. 12, no. 3, pp. 875-890, March 2019
 21. Šiško, J.: *Obrada satelitskih SAR podataka (Satellite SAR data processing)*, graduation thesis, Faculty of Geodesy, Zagreb, 2017
 22. Skolnik, M. I.: *Introduction to radar systems*, 2nd edn. McGraw-Hill, Boston, Mass, 1980
 23. van Zyl, J., Chapman, B. D., Dubois, P. & Shi, J.: The effect of topography on SAR calibration. *IEEE Transactions on Geoscience and Remote Sensing* 31 (5), 1036–1043., 1993
 24. Warren, S., Hahn, C., London, J., Chervin, R. & Jenne, R.: *Global distribution of total cloud cover and cloud type amounts over land*. UCAR/NCAR, NCAR Library, 1986
- LIST OF URLs
- URL 1. <https://sentinel.esa.int/web/sentinel/missions/sentinel-1> (24.5.2021)
- URL 2. <https://asf.alaska.edu/> (24.5.2021)
- URL 3. <https://step.esa.int/main/doc/tutorials/> (23.4.2021)
- URL 4. <https://web.stanford.edu/group/radar/softwareandlinks/sw/snaphu/> (28.6.2021)